

Adaptive Torque Control for Sensorless Induction Motor Drives in Wide-Speed Range

Aleksandar Ž. Rakić

University of Belgrade, School of Electrical Engineering
Belgrade, Serbia
rakic@etf.rs

Petar R. Matić

University of Banja Luka, School of Electrical Engineering
Banja Luka, Republic of Srpska, Bosnia and Herzegovina
pero@etfbl.net

Abstract—In this paper, control structure is proposed to ensure desired performance of sensorless induction motor (IM) drives in both base speed range and field-weakening. Appropriate nonlinear IM model is utilized for derivation of adaptive slip manipulation based torque control law. In the base speed range, proposed solution reduces to indirect field-oriented control (IFOC), while in the field weakening it becomes voltage angle control with full dc bus utilization. Proposed solution is verified by means of simulation.

Keywords - induction motor; sensorless drive; torque control.

I. INTRODUCTION

The high performance IM drives are mainly controlled by field-oriented control schemes [1], where direct torque control (DTC) make immediate use of stator voltage vector to control the torque, while IFOC-type torque control rely on embedded current control loops. During the last decade high-speed IM drives are being in the focus of research [2]-[13] for their efficiency, small cost and the ability to operate in wide speed range without the mechanical transmission gear. The operation of IM at speeds higher than the nominal one is enabled by the field-weakening (reduction of the rotor flux), where maximum torque capability can be obtained only by the full utilization of available inverter voltage, i.e. stator voltage vector is required to be in saturation with its amplitude set to maximal.

Though IFOC obtains superior dynamic performance in base-speed region, proper operation of its current loops in the field-weakening demands absence of the stator voltage saturation. On the other hand, authors of this paper proposed DTC-type voltage angle torque control (VATC) [14]-[17], which is intended for the full DC bus utilization and high performance in the field weakening, while its base-speed region performance is recognized to be inferior to IFOC. In this paper, adaptive torque control solution is proposed as a proper utilization of both IFOC and VATC in the regions of their superiority; IFOC in the base-speed region, and VATC in the field-weakening.

The rest of the paper is organized as follows. In Section II appropriate nonlinear state-space model of IM is presented. Outline of torque control derivation is presented in Section III, along with the structural block diagram of the overall control solution. Verification by simulation in few representative torque demand scenarios is given in Sect. IV.

II. NONLINEAR IM MODEL

Assuming mechanical transients are much slower than electrical ones, the state-space model of the IM, in normalized (per-unit [p.u]) values, is given as follows:

$$\frac{di_d}{dt} = \omega_b \left[-\frac{i_d}{T_\sigma} + \omega_{dq} i_q + \frac{k_r \Psi_D}{T_r L_\sigma} + \omega_r \frac{k_r \Psi_Q}{T_r L_\sigma} + \frac{u_d}{L_\sigma} \right], \quad (1)$$

$$\frac{di_q}{dt} = \omega_b \left[-\omega_{dq} i_d - \frac{i_q}{T_\sigma} - \omega_r \frac{k_r \Psi_D}{L_\sigma} + \frac{k_r \Psi_Q}{T_r L_\sigma} + \frac{u_q}{L_\sigma} \right], \quad (2)$$

$$\frac{d\Psi_D}{dt} = \omega_b \left[\frac{L_m}{T_r} i_d - \frac{1}{T_r} \Psi_D + \omega_{sl} \Psi_Q \right], \quad (3)$$

$$\frac{d\Psi_Q}{dt} = \omega_b \left[\frac{L_m}{T_r} i_q - \omega_{sl} \Psi_D - \frac{1}{T_r} \Psi_Q \right], \quad (4)$$

$$t_e = \frac{L_m}{L_r} (\Psi_D i_q - \Psi_Q i_d), \quad (5)$$

where the state vector consists of stator currents and rotor fluxes, motor torque t_e is primary output variable, and immediate controlling variables are stator voltage components u_d and u_q .

In the model (1) – (5), ω_b is base speed and all other variables and parameters are normalized (in [p.u]): ω_{dq} is synchronous frequency, ω_{sl} is motor slip, ω_r is rotor angular velocity, R_s and R_r are stator and rotor resistance, L_s and L_r are stator and rotor self-inductances, L_m is mutual inductance, $k_r = L_m/L_r$ is rotor coupling coefficient, $T_\sigma = L_\sigma / R_\sigma$ and $T_r = L_r / R_r$ are stator and rotor transient time constants in [p.u], $\sigma = 1 - M^2 / L_s L_r$ is leakage coefficient and l_s is stator inductance in [p.u].

III. PROPOSED TORQUE CONTROL

Performing Laplace transform on (3) and (4), solving the system of equations for $\Psi_D(i_d, i_q)$ and $\Psi_Q(i_d, i_q)$, and introducing the obtained solutions in (5), result in:

$$t_e = \frac{T_r L_m^2}{L_r} \frac{i_d^2 + i_q^2}{T_r^2 p^2 + 2T_r p + 1 + \omega_{sl}^2 T_r^2} \omega_{sl}, \quad (6)$$

where p stands for the complex variable of the Laplace transform.

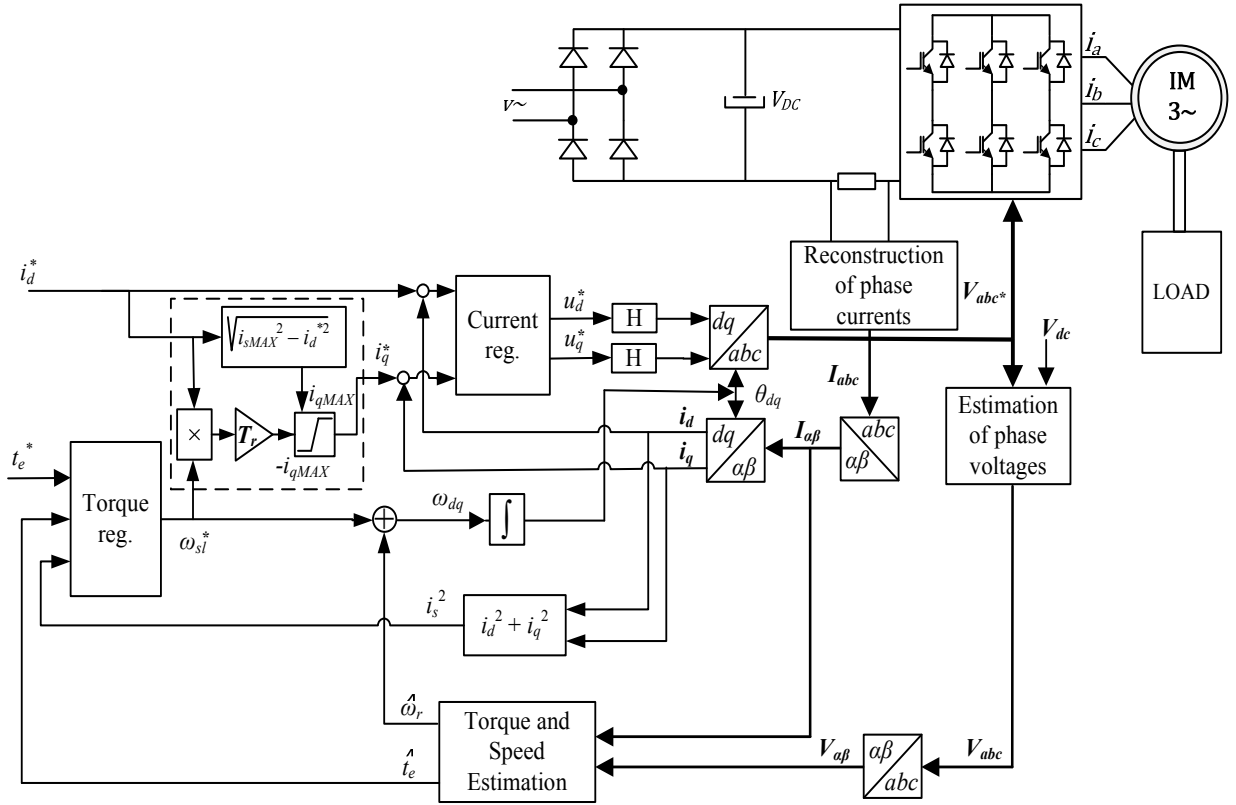


Figure 1. Structural block diagram of the proposed solution

In the vicinity of the operating regime $(\omega_{sl}, i_s) = (\omega_{sl}^0, i_s^0)$, where $i_s = \sqrt{i_d^2 + i_q^2}$ is the stator current modulus, transfer from the control variable ω_{sl} to the output t_e is adopted as a low-frequency approximation of (6):

$$G_0 = \frac{L_m^2}{R_r} \frac{(i_s^0)^2}{1 + (\omega_{sl}^0 T_r)^2}. \quad (7)$$

For the plant (7) and adopted bandwidth

$$\omega_0 = \frac{\omega_b}{T_r}, \quad (8)$$

gain-scheduling integral torque controller is proposed:

$$K(p) = \frac{\omega_0}{G_0} \frac{1}{p}. \quad (9)$$

In order to prevent excessive control actions which could lead to torque breakdown, limit of $\pm 1/(\sigma T_r)$ is set to integration in (9).

Block diagram of proposed torque control method is shown on Fig. 1. The basic idea is to utilize unique torque regulator to perform motor-slip command ω_{sl}^* calculation for both base-speed region (BSR) and field-weakening (FW), since the proposed control law (9) uses model (7), which is valid in both drive operation regimes. When the drive operates in BSR, reference currents i_d^* and i_q^* are fed to current regulators and proposed solution reduces to

effective IFOC algorithm. On the other hand, when output voltage commands u_d^* and u_q^* reach the limit $U_{s \max}$ of maximal available inverter voltage amplitude ($\sqrt{u_d^{*2} + u_q^{*2}} = U_{s \max}$), the output voltage commands u_d^* and u_q^* of the current regulators are held by holding circuits H and drive enters the FW regime. Inverter voltage is fully utilized and the torque control is effectively performed by the stator voltage angle control, i.e. the torque regulator adjusts the angle of the (maximal amplitude) stator voltage vector only by motor-slip manipulation.

Though voltage limit is explicitly addressed by the proposed control solution, the inverter current limit $I_{s \max}$ violations are possible so far. One way to impose the current limitation in torque control is to calculate maximal reachable motor torque in the existing operating regime for the current engagement i_s limited to $I_{s \max}$. Utilizing model (7), maximal reachable motor torque

$$t_{e,LM}^* = \frac{L_m^2 I_{s \max}^2}{R_r} \frac{\omega_{sl}^0}{1 + (\omega_{sl}^0 T_r)^2} \quad (10)$$

can be used as a dynamic limitation of the torque command t_e^* in order to effectively impose the limitation of the motor current.

IV. SIMULATION RESULTS

Simulations were conducted in Matlab/Simulink in order to verify expected performance. Proposed torque control

solution is tested through scenarios of torque command t_e^* application in different IM operating regimes, i.e. BSR and FW, as well as in transition between the aforementioned regimes. Control system is tested without any outer speed or position control loop and torque commands are chosen to be in the form of sequenced step changes. In that way torque control solution is exposed to worst case demands and obtained performance is expected only to be more favorable in the real-time exploitation than in the tested cases (outer control loops would set less demanding t_e^* signal shapes than the adopted step changes). Parameters of tested motor are given in Appendix.

The first test scenario is the sequential bidirectional application of maximal amplitude torque commands. The timing of step changes is chosen to lead the IM from BSR to FW and vice versa several times and in both rotation directions. The responses of all relevant variables are given in Fig. 2. Within first 2 seconds motor is brought from BSR into the FW and quickly returned to BSR. At $t = 2$ sec, maximal positive torque command is applied and it drives motor speed again into the FW and up to 2 p.u. speed in forward direction. At $t = 5$ sec, maximal negative torque command is applied and it first drives motor back to BSR in forward direction and then, at $t \approx 6.8$ sec, reverses the direction of rotation and forces the motor to enter FW in reverse direction and build the speed up to approx. -2 p.u.

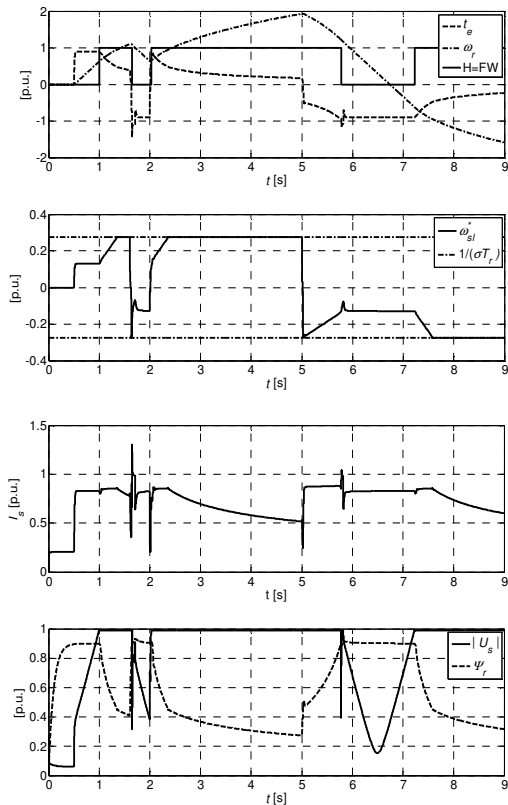


Figure 2. Test scenario with multiple bidirectional transitions to/from field weakening

Voltage saturation in FW results in automatically adjusted (decreased) levels of the rotor flux and obtainable torque, but it influences neither stability nor the performance of the torque control loop. The stator current amplitude is efficiently kept below the $I_{s \max} = 1$ p.u. at all times, except at the FW→BSR transients. The reason of this current limit breach is the initial response of the reactivated IFOC current regulation. The effect is negligible, since $I_{s \max}$ stands for the steady current load limitation and the short-term current overloads are permitted (within the voltage inverter current margin).

The second test scenario is the sequential bidirectional application of 50% amplitude torque commands which keeps the IM in BSR, but drives it in both rotation directions. Wave-forms of the relevant variables are given in Fig. 3. Since both current and voltage are within limits, rotor flux is at its nominal value and the torque command is always fully attained.

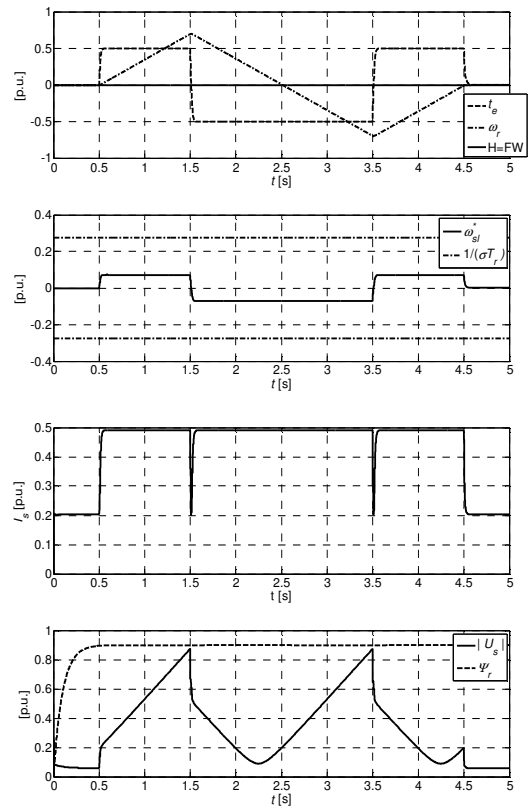


Figure 3. Test scenario for base speed performance evaluation.

Reversing of the drive rotation direction happens at $t = 2.5$ sec. No issues around zero speed were detected in torque or flux, mainly because inverter nonlinearities are neglected in the simulation model. Proposed torque control is primarily intended for high speed mode of operation in order to fully utilize available inverter voltage. However, operation at low speeds and reversing of the real drive is also possible, but with the speed estimation scheme suitable for low speeds.

The third test scenario is the sequential unidirectional application of maximal amplitude torque commands, which leads the drive deep into the FW in forward rotation direction. The responses of all relevant variables are given in Fig. 4. As in the case of the first scenario, voltage limit is reached in the FW region and rotor flux and torque producing capability is decreased. However, the current limit is not being breached, since the current demand in FW only decreases with the increase of drive speed. The quality of all the transients is desired.

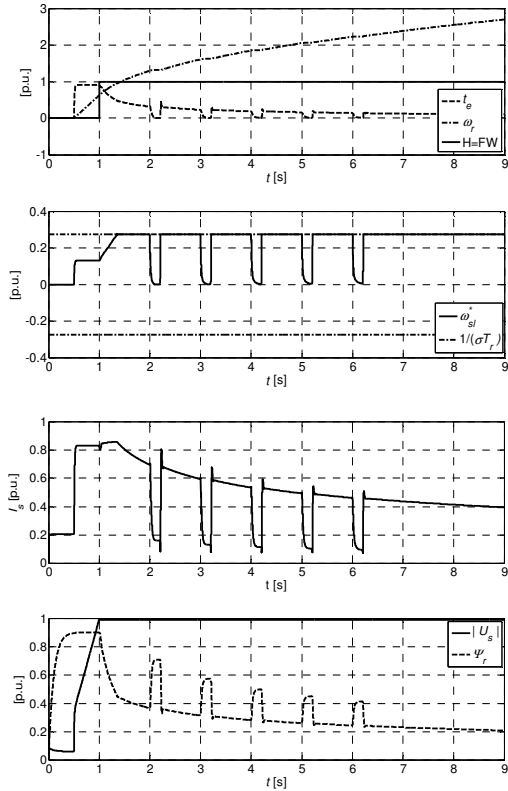


Figure 4. Test scenario for field weakening performance evaluation.

It can be observed in the FW drive operation that the rotor flux automatically regenerates (builds up) and the stator current drops to level lower than in BSR, when the torque demand is absent. This property may lead to conclusion that the proposed torque control represents optimal (or near optimal) solution in the sense of minimal power consumption with maximal torque producing capability, which is worth of the further investigation.

APPENDIX

Motor data: 750W, 195V, 70Hz, $R_s = 10.8\Omega$, $R_r = 5.673\Omega$, $L_s = L_r = 0.552$ H, $L_m = 0.518$ H.

REFERENCES

- [1] D. Casadei, F. Profumo, G. Serra, A. Tani, "FOC and DTC: Two Viable Schemes for Induction Motor Torque Control", *IEEE Transactions on Power Electronics*, Vol. 17, No.5, September 2002, pp. 779-787.
- [2] J. Pyrhonen, J. Nerg, P. Kurrnen, U. Lauber, "High-Speed High-Output Solid-Rotor Induction-Motor Technology for Gas Compression", *IEEE Transactions on Industrial Electronics*, Vol. 57, No.1, January 2010, pp. 272-280.
- [3] M. Centner, U. Schäfer, "Optimized Design of High-Speed Induction Motors in Respect of the Electrical Steel Grade", *IEEE Transactions on Industrial Electronics*, Vol. 57, No.1, January 2010, pp. 288-295.
- [4] J. F. Gieras, J. Saari, "Performance Calculation for a High-Speed Solid-Rotor Induction Motor", *IEEE Transactions on Industrial Electronics*, Vol. 59, No.6, June 2012, pp. 2689 - 2700
- [5] M. Mengoni, L. Yarri, A. Tani, G. Serra, D. Casadei, "Stator Flux Vector Control of Induction Motor Drive in the Field Weakening Region", *IEEE Transactions on Power Electronics*, Vol. 23, No. 2, March 2008, pp. 941-949.
- [6] P. Y. Lin, Y. S. Lai, "Novel Voltage Trajectory Control for Field-Weakening Operation of Induction Motor Drives", *IEEE Transactions on Industry Applications*, Vol. 47, No. 4, January/February 2011, pp. 122-127.
- [7] R. Sepulchre, T. Devos, F. Jadot, F. Malrait, "Antiwindup Design for Induction Motor Control in the Field Weakening Domain", *IEEE Transactions on Control System Technology*, Vol. 21, No.1, January 2013, pp. 52-66.
- [8] F. Briz, A. Diez, M. W. Degner, R. D. Lorenz, "Current and Flux Regulation in Field-Weakening Operation", *IEEE Transactions on Industry Applications*, Vol. 37, No.1, January/February 2001, pp. 42-50.
- [9] G. Gallegos-López, F. S. Gunawan, J. E. Walters, "Current Control of Induction Machines in the Field-Weakened Region", *IEEE Transactions on Industry Applications*, Vol. 43, No.4, July/August 2007, pp. 981-998.
- [10] A. B. Jidin, N. R. B. Idris, A. H. B. M. Yatim, M. E. Elbuluk, T. Sutkino, "A Wide-Speed High Torque Capability Utilizing Overmodulation Strategy in DTC of Induction Machines With Constant Switching Frequency Controller", *IEEE Transactions on Power Electronics*, Vol. 27, No. 5, May 2012, pp. 2566-2575.
- [11] D. Casadei, G. Serra, A. Tani, L. Zari, F. Profumo, "Performance Analysis of a Speed Sensorless Induction Motor Drive Based on a Constant Switching Frequency DTC Scheme", *IEEE Transactions on Industry Applications*, Vol. 39, No. 2, March/April 2003.
- [12] M. Hajian, J. Soltani, G. A. Markadeh, S. Hosseinnia, "Adaptive Nonlinear Direct Torque Control of Sensorless IM Drives With Efficiency Optimization" *IEEE Transactions on Industrial Electronics*, Vol. 57, No.3, March 2010, pp. 975-985.
- [13] J. Rodríguez, R. M. Kennel, J. R. Espinoza, M. Trincado, C. A. Silva, C. A. Rojas, "High-Performance Control Strategies for Electrical Drives: An Experimental Assessment", *IEEE Transactions on Industrial Electronics*, Vol. 59, No.2, February 2012, pp. 812-820.
- [14] P. Matic, A. Rakić, and S. Vukosavić, "Induction Motor Torque Control in Field Weakening by Voltage Angle Control," in Proc. 14th Int. Power Electronics and Motion Control Conf. (EPE/PEMC), Ohrid, Macedonia, Sep. 6-8, 2010, pp. T4-108-T4-115.
- [15] P. Matic, A. Rakić, and S. Vukosavić, "Direct Torque Control of Induction Motor in Field Weakening Based on Gain-Scheduling Approach," in Proc. 16th Int. Symp. Power Electronics (Ee 2011), Novi Sad, Serbia, Oct. 26-28, 2011.
- [16] A. Rakić, P. Matic, "Robust Modeling and Reference Tracking Control of Voltage Angle Controlled Induction Motor in Field Weakening Regime," in Proc. INDEL Conf., Banja Luka, Republic of Srpska - Bosnia and Herzegovina, Nov. 4-6, 2010, pp. 262-267.
- [17] A. Rakić, P. Matic, T. Petrović, "Robust Modeling and Gain-Scheduling Control of the Induction Motor in the Field Weakening Regime," in Proc. LV ETRAN Conf., Banja Vrućica-Teslić, Republic of Srpska - Bosnia and Herzegovina, Jun. 6-9, 2011, pp. AU4.5-1-4.